Analytical Derivative Approaches for Vibro-Polaritonic Structures and Properties I: Formalism and Implementation

Xunkun Huang and WanZhen Liang[a)]

State Key Laboratory of Physical Chemistry of Solid Surfaces,
Collaborative Innovation Center of Chemistry for Energy Materials,
Fujian Provincial Key Laboratory of Theoretical and Computational Chemistry,
and Department of Chemistry, College of Chemistry and Chemical Engineering,
Xiamen University, Xiamen 361005, P. R. China.

Vibro-polaritons are hybrid light-matter states that arise from the strong coupling between the molecular vibrational transitions and the photons in an optical cavity. Developing theoretical and computational methods to describe and predict the unique properties of vibro-polaritons is of great significance for guiding the design of new materials and experiments. Here we present the *ab initio* cavity Born-Oppenheimer density functional theory (CBO-DFT), and formulate the analytic energy gradient and Hessian as well as the nuclear and photonic derivatives of dipole and polarizability within the framework of CBO-DFT to efficiently calculate the harmonic vibrational frequencies, infrared absorption and Raman scattering spectra of vibro-polaritons as well as to explore the critical points on the cavity potential energy surface. The implementation of analytic derivatives into the electronic structure package is validated by comparison with the finite-difference method and with other reported computational results. By adopting appropriate exchange-correlation functionals, CBO-DFT can better describe the structure and properties of molecules in the cavity than CBO-Hartree-Fock method. It is expected that CBO-DFT is a useful tool for studying the polaritonic structures and properties.

[a)]Electronic mail: liangwz@xmu.edu.cn

I. INTRODUCTION

When few (many) molecules are placed in an optical cavity or plasmonic nanocavity, the greatly enhanced coupling between molecular electrons/vibrations and the confined electromagnetic field results in the formation of polariton states and the modification of the physical and chemical properties.[1–6] Vibro-polaritons are created due to the vibrational strong coupling (VSC) of cavity photon and molecular vibrations in which the light-matter coupling is strong enough to exceed the sum of the two parts' dissipation rates, and exhibit modified properties compared to the uncoupled states,[7–10] such as enhancing[11,12] or suppressing[13,14] the rate of chemical reactions, controlling the reaction selectivity.[15–17] In experiments, the formation of vibro-polaritons can be detected by vibrational spectroscopy, including linear infrared (IR) spectra,[18] nonlinear 2-dimensional IR,[19–23] and Raman scattering spectra.[24–27]

The research in this field is advancing rapidly, with experimental techniques being developed to predict and control the formation of vibro-polaritons and with theoretical models and computational methods being developed to describe and predict the behavior of these hybrid states.[28–35] The cavity Born-Oppenheimer approximation (CBOA) provides a theoretical framework to study VSC, in which the nuclei and photon are treated on the equal footing so that spans the cavity potential energy surfaces (CPES).[36,37] Currently there are two types of theoretical methods based on the CBOA which focus on the electronic structure. The time-dependent dynamics methods[38,39] are beyond the subject of this manuscript. The first type (denoted as *ab initio* CBO in this manuscript) focuses on solving electronic eigenstates, including QEDFT,[40] CBO-HF,[41,42] and CBO-CC.[43] Among these methods, the photon displacement coordinate is added as an external parameter like nuclear coordinates, and light-matter interaction is treated self-consistently. Another types of methods (denoted as perturbative CBO in this manuscript) include crude CBOA[44] and CBO-PT.[45,46] In these methods, the light-matter interaction operator is projected onto the bare electronic eigenstates, which can be obtained by conventional quantum chemistry calculations. And the photon-electron interactions are added perturbatively. A main advantage of perturbative CBO methods is that one can just rely on the existing quantum chemistry code, as long as the molecular vibrational normal modes and light-matter interaction matrix elements can be calculated. While for *ab initio* CBO methods, the photon displacement coordinate and the light-matter interaction have to be explicitly added in the electronic structure software

package.

Beyond the energy calculations, one would like to optimize molecular geometries, find reaction pathways, calculate thermal and spectroscopic properties and so on with respect to the CPES. This requires to provide the structural quantities such as the force and the force constant, IR and Raman intensities, etc, which are defined as the energy derivatives with respect to the perturbed parameters.[47,48] The perturbed parameters, such as the applied static electric or magnetic fields or the nuclear and photonic displacements, are the variables on which the resulting CPES for a given theoretical model chemistry depends. For example, the energy gradient and Hessian are given as the first derivatives and the second derivatives of the molecular energy with respect to the nuclear and photonic coordinates, respectively, and the IR/Raman intensities can be computed as the first derivatives of the molecular dipole/polarizability with respect to the nuclear and photonic coordinates. Therefore, formulating analytic energy derivatives with respect to the external perturbed variables yields a wealth of molecular properties. This urges us to implement the analytic energy derivatives with respect to the nuclear, perturbed electric field and photonic degrees of freedom (DOF) into the electronic structure package because the analytic derivative approach is superior to the numerical differentiation method on the computational accuracy and efficiency.[49–51]

The analytic gradient of CBO-HF energy has been formulated and used to calculate vibro-polaritonic IR spectra by Kowalewski et al.[42,52] However the required Hessian in their spectral calculation was obtained by numerically differentiating the energy gradient. Furthermore, the HF ansatz largely overestimates the harmonic frequencies of molecules. Aiming at solving these issues, in this work, we combine the CBOA with the density functional theory (DFT) and develop CBO-DFT approach. Then we formulate the analytical gradient and Hessian of CBO-DFT energy as well as the nuclear and photonic derivatives of dipole and polarizability, and implement these analytic derivatives into the electronic structure package. The successful implementation of analytic derivatives enables us to effectively characterize the linear IR and Raman scattering spectra of vibro-polaritons and understand the unique properties that arise from the strong coupling between vibrational modes and electromagnetic waves. We also implement the procedure of geometry optimization on the CPES so that we can analysis the critical points on the CPES. Furthermore, we compare the geometry and properties of molecule in cavity calculated by CBO-DFT with different exchange-correlation (XC) functionals and CBO-HF, and the results show that CBO-DFT

combined with appropriate XC functionals outperforms CBO-HF in describing the structure and properties of molecules in the cavity.

The manuscript is arranged as follows. In Sec.II, we present the expressions of CBO-DFT energy, energy gradient, and Hessian, and we also rationalize the procedure of calculating the frequencies and spectral intensities of vibro-polaritons. In Sec.III, we show geometry optimization on the CPES, the model Hessian that helps us to understand the features of vibro-polaritonic spectra, comparison between CBO-DFT and CBO-HF, and the *ab initio* vibro-polaritonic spectra of acetone calculated within the framework of the CBO-DFT. Finally, the concluding remarks are summarized in Sec.IV.

II. THEORY

In this manuscript, the subscript A is the index of nuclei, and i the electrons. The subscript n represents the Cartesian components which can be $\{x, y, z\}$. $\{\mu, \nu, \ldots\}$ index the atomic orbitals (AO). The derivative is represented by the superscripts, in which superscript x represents nuclear derivative, q the photon displacement derivative, and n the derivative with respect to electric field component f_n. The superscripts bracketed with '[]' refer to the explicit derivatives excluding the contributions from orbital rotations matrix Θ. The vectors are marked by the arrow above, and matrices as well as vector operators are shown in bold. '$\cdot$' represents dot product of two vectors or two matrices, and the expression $\mathbf{AB}$ is the matrix product of matrix $\mathbf{A}$ and $\mathbf{B}$. The detailed derivations of analytical derivatives shown in this section are presented in the Sec.I of supplementary material.

A. CBO-DFT Energy and Gradients

The usual starting point of polaritonic chemistry is the Pauli-Fierz Hamiltonian (in the length gauge and dipole approximation).[53] In this work, we assume the molecule is coupled with a single cavity mode:

$$\hat{H} = \hat{T}_{\mathrm{nuc}} + \hat{H}_{\mathrm{e}} + \frac{\hat{p}^2}{2} + \frac{1}{2}\omega_{\mathrm{c}}^2\hat{q}^2 - \omega_{\mathrm{c}}(\vec{\lambda}\cdot\hat{\boldsymbol{\mu}})\hat{q} + \frac{1}{2}(\vec{\lambda}\cdot\hat{\boldsymbol{\mu}})^2. \tag{1}$$

$\hat{T}_{\mathrm{nuc}} + \hat{H}_{\mathrm{e}}$ constitutes the molecular Hamiltonian in vacuum. $\frac{1}{2}(\hat{p}^2 + \omega_{\mathrm{c}}^2\hat{q}^2)$ is the photonic Hamiltonian, in which $\hat{p}$ and $\hat{q}$ are photon momentum and displacement operators respectively. $-\omega_{\mathrm{c}}(\vec{\lambda}\cdot\hat{\boldsymbol{\mu}})\hat{q}$ describes the dipolar coupling between molecule and cavity mode, where

$\hat{\boldsymbol{\mu}}$ is the molecular dipole operator, and $\vec{\lambda} = \sqrt{\frac{4\pi}{V}}\vec{e}$ is the coupling vector, in which its magnitude is determined by the effective quantization volume V of cavity, and $\vec{e}$ is the unit vector representing the polarization direction. The last term $\frac{1}{2}(\vec{\lambda}\cdot\hat{\boldsymbol{\mu}})^2$ is the so-called dipole self-energy operator, and it ensures the light-matter system to have a ground state.[54]

In the VSC regime, the cavity electromagnetic mode is coupled to molecular vibrational degrees of freedom. The CBOA provides a theoretical framework to describe VSC. At this stage, the nuclear and photonic kinetic operators are separated from the PF Hamiltonian, and we treat the nuclear coordinates $\mathbf{R}$ and photon displacement coordinate q as external parameters instead of operators. This results in the CBO Hamiltonian

$$\hat{H}_{\mathrm{CBO}} = \hat{H}_{\mathrm{e}}(\mathbf{R}) + \frac{1}{2}\omega_{\mathrm{c}}^2 q^2 - \omega_{\mathrm{c}}(\vec{\lambda}\cdot\hat{\boldsymbol{\mu}})q + \frac{1}{2}(\vec{\lambda}\cdot\hat{\boldsymbol{\mu}})^2, \tag{2}$$

and also defines the CPES, $E_{\mathrm{CBO}}(\mathbf{R}, q)$. Note that the molecular dipole operator is now $\hat{\boldsymbol{\mu}} = \vec{\mu}_{\mathrm{nuc}} + \hat{\boldsymbol{\mu}}_{\mathrm{e}} = \sum_A Z_A\vec{R}_A - \sum_i \hat{\mathbf{r}}_i$, where Z_A and $\vec{R}_A$ are the charge and coordinates of the A-th nuclei, and $\hat{\mathbf{r}}_i$ is the coordinate operator of the i-th electron.

In this work, the electron-electron correlation effects are covered by the density functional theory (DFT). This combination of CBOA with DFT is called as CBO-DFT here. Unlike QEDFT, CBO-DFT does not construct the generally unknown exchange-correlation functional to account for the photon-electron correlation. It adopts the standard DFT XC functionals, employed in conventional quantum chemistry code. The CBO-DFT ground state is described by a single determinant of Kohn-Sham orbitals, and the corresponding expression of energy in atomic orbital (AO) representation can be written as[41,53]

$$\begin{aligned} E_{\mathrm{CBO}}(\mathbf{R}, q) = E_{\mathrm{e}}(\mathbf{R}) &+ \frac{1}{2}\omega_{\mathrm{c}}^2 q^2 - \omega_{\mathrm{c}} q\vec{\lambda}\cdot\vec{\mu} \\ &+ \frac{1}{2}(\vec{\lambda}\cdot\vec{\mu})^2 + \mathbf{q}\cdot\mathbf{P} - \frac{1}{2}\mathbf{P}\cdot(\mathbf{dPd}). \end{aligned} \tag{3}$$

Here $E_{\mathrm{e}}(\mathbf{R}) = \mathbf{P}\cdot(\mathbf{h} + \frac{1}{2}\boldsymbol{\Pi}\cdot\mathbf{P}) + E_{\mathrm{xc}} + V_{\mathrm{nuc}}$ is the usual electronic energy of the molecules in vacuum. $\mathbf{P}$ is the reduced one-electronic density matrix, and $\mathbf{h}$ is the core Hamiltonian. The two-electron integral supermatrix $\boldsymbol{\Pi}$ in atomic basis is $\Pi_{\mu\nu,\lambda\sigma} = (\mu\nu|\lambda\sigma) - c_{\mathrm{HFX}}(\mu\lambda|f(\vec{r}_{12})|\nu\sigma)$, adopting approximate coefficient c_{HFX} and operator $f(\vec{r}_{12})$ for hybrid and range-separated functionals. Furthermore E_{xc} is the DFT exchange-correction energy and V_{nuc} is the nuclear repulsion energy. $\vec{\mu} = \vec{\mu}_{\mathrm{nuc}} + \vec{\mu}_{\mathrm{e}}$ is the expectation value of the molecular dipole moment, and its n-direction component is $\mu_n = \sum_A Z_A R_{A,n} - \mathbf{P}\cdot\mathbf{M}_n$, in which the n-component of the dipole matrix in AO basis is $M_{n,\mu\nu} = \int \chi_\mu(\vec{r}) r_n \chi_\nu(\vec{r})\,\mathrm{d}\vec{r}$. The compact

expression of the expectation value of dipole self-energy operator includes the last three terms in Eq.(3). Using the fact that $(\sum_i \vec{\lambda}\cdot\hat{\mathbf{r}}_i)^2 = \sum_i(\vec{\lambda}\cdot\hat{\mathbf{r}}_i)^2 + \frac{1}{2}\sum_{i\neq j}[(\vec{\lambda}\cdot\hat{\mathbf{r}}_i)(\vec{\lambda}\cdot\hat{\mathbf{r}}_j) + (\vec{\lambda}\cdot\hat{\mathbf{r}}_j)(\vec{\lambda}\cdot\hat{\mathbf{r}}_i)]$, the concrete expression is

$$\begin{aligned}\frac{1}{2}\langle(\vec{\lambda}\cdot\hat{\boldsymbol{\mu}})^2\rangle = \frac{1}{2}(\vec{\lambda}\cdot\vec{\mu}_{\mathrm{nuc}})^2 + (\vec{\lambda}\cdot\vec{\mu}_{\mathrm{nuc}})(\vec{\lambda}\cdot\vec{\mu}_{\mathrm{e}}) + \sum_{\mu\nu} q_{\mu\nu}P_{\mu\nu} \\ + \frac{1}{2}\sum_{\mu\nu\lambda\sigma} P_{\mu\nu}d_{\mu\nu}d_{\lambda\sigma}P_{\lambda\sigma} - \frac{1}{2}\sum_{\mu\nu\lambda\sigma} P_{\mu\nu}d_{\mu\sigma}d_{\lambda\nu}P_{\lambda\sigma}.\end{aligned} \tag{4}$$

Here we define the matrix $d_{\mu\nu} = \sum_n \lambda_n M_{n,\mu\nu}$, and the matrix $q_{\mu\nu} = \frac{1}{2}\sum_{mn}\lambda_m Q_{mn,\mu\nu}\lambda_n$ in which the element of quadrupole matrix is $Q_{mn,\mu\nu} = \int \chi_\mu(\vec{r}) r_m r_n \chi_\nu(\vec{r})\,\mathrm{d}\vec{r}$. Note that $\sum_{\mu\nu} P_{\mu\nu}d_{\mu\nu} = -\vec{\lambda}\cdot\vec{\mu}_{\mathrm{e}}$, then Eq.(4) can be simplified to its form in Eq.(3). The Fock matrix within CBO-DFT is

$$\mathbf{F} = \mathbf{h} + \boldsymbol{\Pi}\cdot\mathbf{P} + \mathbf{V}_{\mathrm{xc}}(\mathbf{P}) + (\omega_{\mathrm{c}}q - \vec{\lambda}\cdot\vec{\mu}_{\mathrm{nuc}})\mathbf{d} + \mathbf{q} + \mathbf{d}(\mathbf{d}\cdot\mathbf{P}) - \mathbf{dPd}. \tag{5}$$

The nuclear gradients of CBO-DFT energy can be derived via the Lagrangian approach.[55] The CBO-DFT Lagrangian is defined as $L_{\mathrm{CBO}} = E_{\mathrm{CBO}} - \sum_{pq}\varepsilon_{pq}(S_{pq} - \delta_{pq})$, in which the subscripts $\{p, q\}$ index the molecular orbitals. $\mathbf{S}$ is the overlap matrix and $\boldsymbol{\varepsilon}$ is the Lagrange multiplier. The derivative of CBO energy with respect to nuclear coordinate x is therefore the partial derivative of energy Lagrangian

$$\begin{aligned}E^x_{\mathrm{CBO}} &= \frac{\mathrm{d}E_{\mathrm{CBO}}}{\mathrm{d}x} = \frac{\partial L_{\mathrm{CBO}}}{\partial x} \\ &= \mathbf{h}^{[x]}\cdot\mathbf{P} + \frac{1}{2}\mathbf{P}\cdot\boldsymbol{\Pi}^{[x]}\cdot\mathbf{P} + E^{[x]}_{\mathrm{xc}} + V^{[x]}_{\mathrm{nuc}} - \mathbf{W}\cdot\mathbf{S}^{[x]} \\ &\quad + (\vec{\lambda}\cdot\vec{\mu} - \omega_{\mathrm{c}}q)(\vec{\lambda}\cdot\vec{\mu}^{[x]}_{\mathrm{nuc}} - \mathbf{d}^{[x]}\cdot\mathbf{P}) + \mathbf{q}^{[x]}\cdot\mathbf{P} - \mathbf{P}\cdot(\mathbf{dPd}^{[x]}),\end{aligned} \tag{6}$$

in which $W_{\mu\nu} = (\mathbf{PFP})_{\mu\nu}$ and it is called energy weighted density matrix. Since there is one new dimension, the photon displacement coordinate q, the gradient with respect to it is also required. The Lagrangian approach is also applied, but in this case the constraint term does not explicitly depend on q. The expression of photonic gradient is

$$E^q_{\mathrm{CBO}} = \frac{\partial L_{\mathrm{CBO}}}{\partial q} = \omega_{\mathrm{c}}^2 q - \omega_{\mathrm{c}}\vec{\lambda}\cdot\vec{\mu}. \tag{7}$$

B. CBO-DFT Hessian

The second derivative of CBO-DFT energy is essential for calculating harmonic vibrational spectra, and exploring the critical points of CPES. The analytical expression of Hessian is obtained by directly differentiating the gradient. The photon-photon Hessian and

photon-molecule Hessian are easy to get:

$$E^{qq}_{\mathrm{CBO}} = \omega_{\mathrm{c}}^2 - \omega_{\mathrm{c}}\vec{\lambda}\cdot\vec{\mu}^q, \tag{8}$$

$$E^{qx}_{\mathrm{CBO}} = -\omega_{\mathrm{c}}\vec{\lambda}\cdot\vec{\mu}^x. \tag{9}$$

In both parts, the derivatives of total dipole are involved. The nuclear derivative of dipole is $\mu_n^x = \sum_A Z_A R_{A,n}^{[x]} - \mathbf{M}_n\cdot\mathbf{P}^x - \mathbf{M}_n^{[x]}\cdot\mathbf{P}$ and photonic derivative of dipole is $\mu_n^q = -\mathbf{M}_n\cdot\mathbf{P}^q$. And the expression of Hessian with respect to nuclear displacement is

$$\begin{aligned} E^{xy}_{\mathrm{CBO}} = {} & \mathbf{h}^{[xy]}\cdot\mathbf{P} + \frac{1}{2}\mathbf{P}\cdot\mathbf{\Pi}^{[xy]}\cdot\mathbf{P} + E_{\mathrm{xc}}^{[xy]} + V_{\mathrm{nuc}}^{[xy]} \\ & - (\vec{\lambda}\cdot\vec{\mu} - \omega_{\mathrm{c}}q)\mathbf{d}^{[xy]}\cdot\mathbf{P} + (\vec{\lambda}\cdot\vec{\mu}_{\mathrm{nuc}}^{[y]} - \mathbf{d}^{[y]}\cdot\mathbf{P})(\vec{\lambda}\cdot\vec{\mu}_{\mathrm{nuc}}^{[x]} - \mathbf{d}^{[x]}\cdot\mathbf{P}) \\ & + \mathbf{q}^{[xy]}\cdot\mathbf{P} - \mathbf{P}\cdot(\mathbf{d}\mathbf{P}\mathbf{d}^{[xy]}) - \mathbf{P}\cdot(\mathbf{d}^{[y]}\mathbf{P}\mathbf{d}^{[x]}) \\ & + \mathbf{F}^{[x]}\cdot\mathbf{P}^y - \mathbf{W}^y\cdot\mathbf{S}^{[x]} - \mathbf{W}\cdot\mathbf{S}^{[xy]}. \end{aligned} \tag{10}$$

The derivative of energy weighted density matrix is

$$\mathbf{W}^y = \mathbf{P}^y\mathbf{F}\mathbf{P} + \mathbf{P}\mathbf{F}\mathbf{P}^y + \mathbf{P}\mathbf{F}^y\mathbf{P}, \tag{11}$$

and the Fock matrix derivative is

$$\mathbf{F}^y = \mathbf{F}^{[y]} + \mathbf{\Pi}\cdot\mathbf{P}^y + \mathbf{V}_{\mathrm{xc}}(\mathbf{P}^y) + \mathbf{d}(\mathbf{d}\cdot\mathbf{P}^y) - \mathbf{d}\mathbf{P}^y\mathbf{d}. \tag{12}$$

In the above expressions, the derivatives of density matrix $\mathbf{P}^x$ and $\mathbf{P}^q$ are required. To calculate them, the derivative of orbital rotations matrix $\Theta^{[x]}$ and $\Theta^{[q]}$ are obtained by solving the coupled-perturbed self-consistent field (CPSCF) equations with respect to nuclear displacement and photon displacement.[56,57] Besides, the orbital response $\Theta^{[n]}$ to electric field perturbation f_n is also solved, which gives us $\mathbf{P}^n$.

To calculate Raman scattering intensity, the derivative of polarizability is required. The expression of polarizability is $\alpha_{mn} = \frac{\partial\mu_m}{\partial f_n} = -\mathbf{M}_m\cdot\mathbf{P}^n$, in which f_n is the electric field along n-direction. And its derivatives with respect to x and q are $\alpha_{mn}^x = -\mathbf{M}_m\cdot\mathbf{P}^{nx}$ and $\alpha_{mn}^q = -\mathbf{M}_m\cdot\mathbf{P}^{nq}$. Thanks to the $2n+1$ rule, the second derivative of density matrix can be calculated only using the first-order orbital response.[58,59] The details of derivations are shown in the supplementary material.

C. Harmonic Frequencies and Spectral Intensities

In this work, the procedure for calculating the harmonic frequencies of vibro-polaritons and the corresponding vibro-polaritonic normal modes is as follows. The Hessian matrix

is converted to the mass-weighted Hessian (MWH) matrix: $H_{\mathrm{m},xy} = E^{xy}_{\mathrm{CBO}}/\sqrt{M_x M_y}$, $g_x = E^{qx}_{\mathrm{CBO}}/\sqrt{M_x}$, and $H_{\mathrm{c}} = E^{qq}_{\mathrm{CBO}}$. M_x represents the mass of the x-th atom, and the "photon mass" is assumed to be 1 a.u. so that we do not show it explicitly. This gives us a MWH matrix with size of $(3N+1) \times (3N+1)$, and the matrix has four blocks

$$\begin{pmatrix} \mathbf{H}_{\mathrm{m}} & \mathbf{g} \\ \mathbf{g}^{\dagger} & \mathbf{H}_{\mathrm{c}} \end{pmatrix}. \tag{13}$$

We first diagonalize the molecule part $\mathbf{H}_{\mathrm{m}}$

$$\mathbf{L}'^{\dagger}\mathbf{D}^{\dagger}\mathbf{H}_{\mathrm{m}}\mathbf{D}\mathbf{L}' = \omega'^{2}_{\mathrm{m}}. \tag{14}$$

Here $\mathbf{D}$ is the projection matrix (following the Eckart conditions[60]) that projects out the translational and rotational normal modes of molecule, and $\mathbf{L}'$ is the mass-weighted vibrational normal coordinate matrix. In this step, we solve $3N-6$ (or $3N-5$ for linear molecules) effective vibrational normal modes of the molecule embedded in the cavity that are ready to be mixed with cavity mode (, and the corresponding spectral intensities are calculated if needed). Next we build the unitary matrix

$$\mathbf{U} = \begin{pmatrix} \mathbf{D}\mathbf{L}' & 0 \\ 0 & 1 \end{pmatrix}, \tag{15}$$

and use it to transform the original MWH matrix into an intermediate MWH matrix

$$\tilde{\mathbf{H}} = \mathbf{U}^{\dagger} \begin{pmatrix} \mathbf{H}_{\mathrm{m}} & \mathbf{g} \\ \mathbf{g}^{\dagger} & \mathbf{H}_{\mathrm{c}} \end{pmatrix} \mathbf{U} = \begin{pmatrix} \omega'^{2}_{\mathrm{m},1} & 0 & \dots & g'_1 \\ 0 & \omega'^{2}_{\mathrm{m},2} & \dots & g'_2 \\ \vdots & \vdots & \ddots & \vdots \\ g'_1 & g'_2 & \dots & \omega'^{2}_{\mathrm{c}} \end{pmatrix}, \tag{16}$$

in which g'_k is the effective coupling of molecule normal mode k with cavity mode and $\omega'^{2}_{\mathrm{c}} = E^{qq}_{\mathrm{CBO}}$. Finally we diagonalize $\tilde{\mathbf{H}}$, i.e. $\mathbf{X}^{\dagger}\tilde{\mathbf{H}}\mathbf{X} = \omega^2$, to get the harmonic frequencies of vibro-polaritonic states, and the vibro-polaritonic normal coordinate matrix is $\mathbf{L} = \mathbf{U}\mathbf{X}$. $\mathbf{L}$ is a matrix of size $(3N+1) \times (3N-5)$, or $(3N+1) \times (3N-4)$ for linear molecule, in which each column describes the portions of molecule characteristic and photon characteristic. The k-th vibro-polaritonic normal coordinate $Q_k = \sum_x L_{x,k}\sqrt{M_x}R_x + L_{3N+1,k}q$, and we use $|L_{3N+1,k}|^2$ to represent the photon characteristic of vibro-polaritonic normal mode k.

The IR spectral intensity I_k of vibro-polaritonic mode k is proportional to $|\vec{\mu}^{Q_k}|^2$, in which $\vec{\mu}^{Q_k}$ is the derivative of total dipole with respect to the vibro-polaritonic normal coordinate Q_k and can also be interpreted as the transition dipole of mode k

$$\vec{\mu}^{Q_k} = \frac{\partial \vec{\mu}}{\partial Q_k} = \sum_{x=1}^{3N} L_{x,k} \frac{\vec{\mu}^x}{\sqrt{M_x}} + L_{3N+1,k} \vec{\mu}^q. \tag{17}$$

The polarizability derivative of normal coordinate Q_k is

$$\alpha_{mn}^{Q_k} = \frac{\partial \alpha_{mn}}{\partial Q_k} = \sum_{x=1}^{3N} L_{x,k} \frac{\alpha_{mn}^x}{\sqrt{M_x}} + L_{3N+1,k} \alpha_{mn}^q. \tag{18}$$

The expression of Raman activity S_k is quite lengthy, and readers can refer to it in the Eq.43 of Ref. 61.

The treatment proposed in this section is due to the following two reasons. Because the translational and rotational normal modes that include photon displacement coordinate may not be well-defined, the projection only applies to the molecule part of MWH matrix. And the intermediate MWH matrix $\tilde{\mathbf{H}}$ in Eq.16 can give us a clear picture of how each molecular vibration interacts with the cavity mode.

III. RESULTS AND DISCUSSIONS

A. Efficiency of Implementation

The CBO-DFT method and its analytic derivatives (including gradient and Hessian) are implemented in a local version of Q-Chem package[62] based on the existing DFT energy derivatives. The procedures of geometry optimization on the CPES, including full optimization and optimization of q with fixed nuclear configuration, are also implemented based on the libopt3 driver. The validations of the implementation of analytic Hessian are shown in the Sec.II of supplementary material where the comparisons to the finite-difference method is made. As shown in Table S1, there is small difference with an error less than 1×10^{-6} between the Hessian calculated by the current analytical derivative and the finite-difference method for water molecule.

To further check the correctness of our calculated spectra, we use the spectra reported by Fischer et al.[46] as the reference. In their article, they calculated the vibro-polaritonic IR spectra of CO_2 and $Fe(CO)_5$ using the CBO-PT(2) method they proposed. To get

closer to their results, we adopt the coordinates of CO_2 and $Fe(CO)_5$ from their article and do not re-optimize them (but we should optimize q, and the optimal values of q are zero for both molecules). The remaining parameters are the same as those in Fischer's article: $\omega_c = 2400\,\mathrm{cm}^{-1}$ and $\vec{\lambda} = (0, 0, 0.03)$ for CO_2, while $\omega_c = 2052\,\mathrm{cm}^{-1}$ and $\vec{\lambda} = (0, 0.03, 0)$ for $Fe(CO)_5$; the FWHM is set $41\,\mathrm{cm}^{-1}$ for Lorentz broadening function. The CBO-DFT calculations are performed using TPSSh[63]/def2-TZVP (note that in Fischer's work, the static polarizability is calculated using CAM-B3LYP[64]/def2-TZVP, which is different from our calculations).

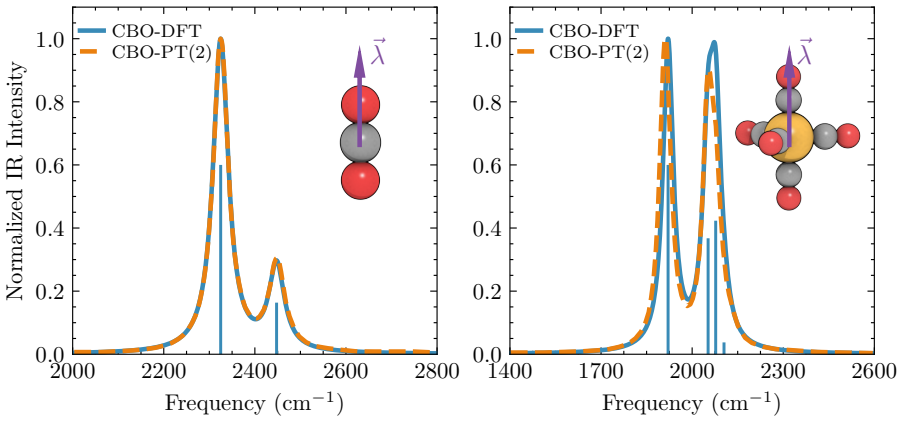

FIG. 1. The linear vibro-polaritonic IR spectra of CO_2 (left) and $Fe(CO)_5$ (right) coupled with a single cavity mode calculated by CBO-DFT and CBO-PT(2).

The calculated IR and Raman spectra of vibrational polaritons by CBO-DFT and CBO-PT(2) are shown in Fig.1. The CBO-PT(2) spectra data are extracted from Fig.2a and Fig.2d of Ref. 46 And for the convenience of comparison, we normalize all spectral curves. In the case of CO_2, our CBO-DFT spectrum is well superposed with the reference CBO-PT(2) spectrum. In the case of $Fe(CO)_5$, on the whole, the CBO-DFT spectrum is also close to the reference CBO-PT(2) spectrum, but with a deviation in the range of $2052\,\mathrm{cm}^{-1}$ to $2077\,\mathrm{cm}^{-1}$. In fact, even though the vibrational modes with frequency of $2052\,\mathrm{cm}^{-1}$ and $2077\,\mathrm{cm}^{-1}$ are purely molecular characteristic which do not couple with cavity mode, in our CBO-DFT calculations, they are influenced indirectly due to the existence of cavity modes (via the dipolar coupling operator and dipole self-energy operator). So the IR intensities may deviate from the reference results in which the parameters are obtained from the quantum chemical calculations of the $Fe(CO)_5$ molecule out-of-cavity. These comparisons can validate

our implementation of analytical derivatives.

B. Geometry Optimization on CPES

The geometry optimization on the CPES involves the nuclear and photonic DOFs. For a fixed nuclear configuration, the CBO-DFT (and CBO-HF) minimum energy is translational invariant if the photon displacement coordinate q is allowed to be re-optimized to fulfill the zero transverse electric field condition.[41] However, the rotational DOFs of the molecules (i.e. the reorientation of molecules with respect to the direction of $\vec{\lambda}$) would lead to a global minimum by minimizing the dipole self-energy. If geometry optimization is performed using Cartesian coordinates, both translational and rotational DOFs are preserved. And in the recent works of Kowalewski[52] and DePrince,[65] rotational DOF is included in the geometry optimizations. In contrast, using internal coordinates prevents the translation and rotation of molecules during geometry optimization so that the optimized configuration may not be a global minimum point. On the other hand, for the theoretical purposes, one would also like to fix the relative orientation of molecule with respect to the cavity polarization direction, as shown in another recent study by Shuai *el al.*[66] Here, we aim to explain how the molecular and photon contributions are combined into the spectral intensities of vibro-polariton theoretically. We thus adopt internal coordinates so that we can fix the relative orientation between molecular vibrational transition dipole and cavity polarization direction.

We follow the strategy that has been used in the QM/MM geometry optimization,[67] in which the molecule uses internal coordinates (delocalized internal coordinates or redundant internal coordinates), while q is in another group of coordinates. A brief description of the definition of mixed coordinates is presented in the Sec. III A of supplementary material. Since the CPES along the q direction is usually much smoother than along the nuclear DOFs, quasi-Newton methods (e.g. BFGS algorithm) are recommended. Fig.2 shows geometry optimization of HF molecule in the cavity. The theoretical level of CPES is B3LYP[68]/aug-cc-pVDZ[69], and the strength of coupling vector $\lambda = 0.05$ (in atomic unit, as $1\,\text{a.u.} = 1\,\sqrt{m_\text{e}}E_\text{h}/e\hbar$) with the direction parallel to the H−F bond. The initial bond length and q are $0.8\,\text{Å}$ and $-4.9\,\text{a.u.}$ respectively. With an exact initial Hessian (orange line) or guess initial Hessian (blue line), the full geometry optimizations all converge to the local minimum, and convergence is faster using the exact initial Hessian.

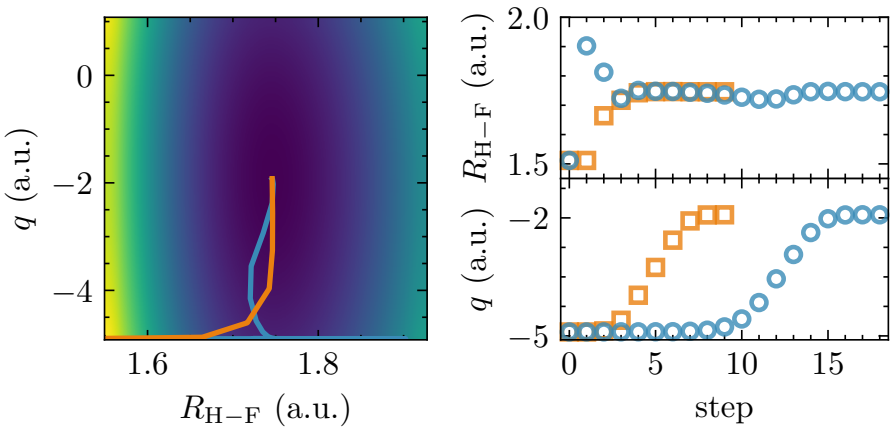

FIG. 2. Left panel displays the trajectories of geometry optimization of HF molecule on the CPES. Right panel displays the H−F bond length and the value of q varied with the number of optimization steps. Orange and blue colors represent the geometry optimization using exact and approximate initial Hessian, respectively.

Additionally, we also compare the geometry optimization results of HF molecule coupled with a single cavity mode using internal coordinates and Cartesian coordinate. Three different initial relative orientation of H−F bond and coupling vector $\vec{\lambda}$, in which the angles between H−F bond and $\vec{\lambda}$ are 0°, 40°, and 90°. The results are summarized in the Sec. III B of supplementary material. In all cases, the optimized HF molecule is perpendicular to the λ which has the lowest energy in Cartesian coordinates regardless of the initial orientation. In contrast, the relative orientations are always kept in internal coordinates.

C. Influence of DFT XC Functionals on Vibro-Polaritonic Spectra

In this section we check how the DFT XC functionals will affect the calculated vibro-polaritonic IR spectra although CBO-DFT doesn't account for the explicit photon-electron correlation in the XC functionals. We consider the single hydrogen fluoride (HF) molecule coupled with a single cavity mode whose polarization direction is aligned with molecular axis. Vibro-polaritonic spectra are calculated using CBO-HF and CBO-DFT with PBE,[70] B3LYP, and ωB97X-V[71] functional. The aug-cc-pVDZ basis set is used in all calculations. First the geometry, harmonic frequency, and dipole of HF molecule out-of-cavity are investigated, and the results are summarized in the above part of Table.I. In this example, the values produced

by B3LYP and ωB97X-V are closest to the experimental one. In contrast, HF method largely overestimates the harmonic frequency and dipole moment, while PBE underestimates these. Since the coupling with cavity mode is mainly through the dipolar coupling (in dipole approximation), accurate calculation of molecular dipole moment is very important. And the dipole moment accuracy of tested methods is consistent with the benchmark results.[72] In the VSC regime, the molecule vibrations are coupled to cavity photon, so precise calculation of vibration frequencies is required. It is obvious that B3LYP and ωB97X-V also outperform HF method at this point.

	R (Å)	ω_{m} (cm^{-1})	μ (debye)
HF	0.9002	4467.2	1.8986
PBE	0.9340	3951.5	1.7585
B3LYP	0.9257	4070.8	1.8026
ωB97X-V	0.9238	4108.9	1.8060
Expt.	0.9168	4138	1.7965
CBO-HF	0.8989	4492.6	1.9042
CBO-PBE	0.9321	3985.1	1.7690
CBO-B3LYP	0.9239	4102.0	1.8119
CBO-ωB97X-V	0.9222	4138.6	1.8144

TABLE I. The calculated bond length R, harmonic frequency ω_{m}, and dipole μ of HF molecule. The aug-cc-pVDZ basis set is used. The experimental data are from Ref. 73.

Then the HF molecule in the cavity is calculated. The coupling strength is set to 0.05 a.u., and the cavity frequency ω_{c} is set to the out-of-cavity molecule vibration frequency for each method correspondingly. The geometry of HF and photon displacement coordinate q are all optimized, followed by spectra calculation. From the below part of Table.I, we can see the properties of HF molecule in the cavity show similar change in all tested methods. The bond length decreases and the effective vibration frequency increases for about $30\,\mathrm{cm}^{-1}$. And the HF molecule is slightly more polar in the cavity. Based on these results, we would expect CBO-DFT provide a better description for molecule part than CBO-HF if an appropriate XC functional is used. The vibro-polaritonic IR spectra are shown in Fig.3, broadened by

a Lorentzian function with a width of $10\,\mathrm{cm}^{-1}$. The overall spectral lineshapes calculated by CBO-DFT and CBO-HF are similar, with the intensity of LP being stronger than that of UP, as predicted by the model Hessian in the previous section. Since the parameters calculated by B3LYP and ωB97X-V are similar, the resulting spectra of them are also close. Due to the overestimation of the vibration frequency by HF method, the positions of peaks predicted by CBO-HF are also located at the higher frequency range. Therefore by adopting an appropriate XC functional in CBO-DFT calculations, the cavity frequency can be naturally set to a more realistic value to match the experimental setup.

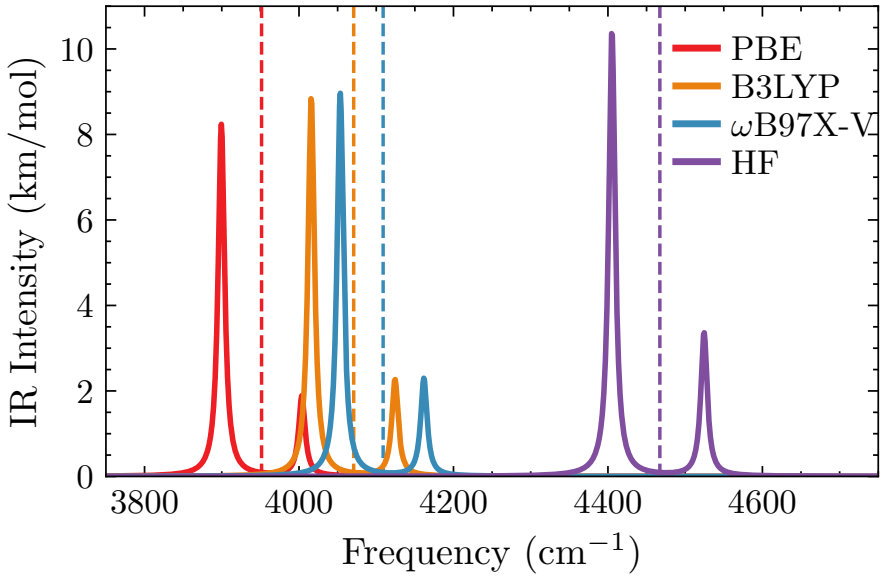

FIG. 3. Vibro-polaritonic IR spectra of a single HF molecule with the coupling strength being 0.05 a.u. calculated by CBO-HF and CBO-DFT. The dashed lines represent the harmonic frequencies of HF molecule out-of-cavity.

IV. CONCLUSIONS

By combining the CBOA with DFT, we have developed the CBO-DFT approach. Subsequently, we have formulated the analytical energy gradient and Hessian as well as the nuclear and photonic derivatives of dipole and polarizability within the framework of CBO-DFT. In addition, the geometry optimization on the CPES which involves nuclear and photonic DOFs has also been implemented. The implementation of analytical Hessian is validated by comparing with finite-difference method, and the IR spectra calculated by CBO-DFT are

verified by comparing to the reported CBO-PT(2) results. Geometry optimization on the CPES using internal coordinates and Cartesian coordinates are compared, and using internal coordinates will keep the orientation of molecule while using Cartesian coordinates can reorient the molecule to reach a lower energy minimum point. The successful implementation of these analytical derivatives and geometry optimization procedure into the electronic structure software package enables us to effectively calculate the geometric and spectral properties of vibro-polaritons and explore the critical points of CPES for the relative large systems. We compare the structures and properties predicted by CBO-DFT and CBO-HF. Compared to the experimental results, CBO-DFT outperforms CBO-HF. We expect CBO-DFT to be a useful tool for studying the polaritonic structures and properties in the VSC regime. And in the next work (Paper II),[74] we will apply the CBO-DFT method to study more realistic and larger molecules, and try to investigate the signatures of calculated vibro-polaritonic spectra.

SUPPLEMENTARY MATERIAL

The supplementary material contains the detailed derivations of analytical derivatives of CBO-DFT energy, definition of mixed coordinate used in geometry optimization, and comparison of internal coordinates and Cartesian coordinates.

ACKNOWLEDGMENTS

The financial support from the National Natural Science Foundation of China (Grant Nos. 22173074 and 22473091) is grateful.

DATA AVAILABILITY STATEMENT

The data that support the findings of this study are available within the article and its supplementary material.

REFERENCES

[1]R. J. Thompson, G. Rempe, and H. J. Kimble, "Observation of normal-mode splitting for an atom in an optical cavity," Phys. Rev. Lett. **68**, 1132–1135 (1992).

[2]R. Miller, T. E. Northup, K. M. Birnbaum, A. Boca, A. D. Boozer, and H. J. Kimble, "Trapped atoms in cavity QED: Coupling quantized light and matter," J. Phys. B: At. Mol. Opt. Phys. **38**, S551 (2005).

[3]B. M. Weight, X. Li, and Y. Zhang, "Theory and modeling of light-matter interactions in chemistry: Current and future," Phys. Chem. Chem. Phys. **25**, 31554–31577 (2023).

[4]B. S. Simpkins, A. D. Dunkelberger, and I. Vurgaftman, "Control, modulation, and analytical descriptions of vibrational strong coupling," Chem. Rev. **123**, 5020–5048 (2023).

[5]X. Huang, W. Zhang, and W. Liang, "Time-dependent Kohn-Sham electron dynamics coupled with nonequilibrium plasmonic response via atomistic electromagnetic model," J. Chem. Phys. **160**, 214106 (2024).

[6]X. Huang and W. Liang, "Real-time simulation of ultrafast electronic dynamics of nanoscale systems involving an organic molecule and a nanoparticle dimer," J. Phys. Chem. Lett. **15**, 6592–6597 (2024).

[7]K. Nagarajan, A. Thomas, and T. W. Ebbesen, "Chemistry under vibrational strong coupling," J. Am. Chem. Soc. **143**, 16877–16889 (2021).

[8]F. J. Garcia-Vidal, C. Ciuti, and T. W. Ebbesen, "Manipulating matter by strong coupling to vacuum fields," Science **373**, eabd0336 (2021).

[9]T. E. Li, B. Cui, J. E. Subotnik, and A. Nitzan, "Molecular polaritonics: Chemical dynamics under strong light-matter coupling," Annu. Rev. Phys. Chem. **73**, 43–71 (2022).

[10]W. Xiong, "Molecular vibrational polariton dynamics: What can polaritons do?" Acc. Chem. Res. **56**, 776–786 (2023).

[11]J. Lather and J. George, "Improving enzyme catalytic efficiency by co-operative vibrational strong coupling of water," J. Phys. Chem. Lett. **12**, 379–384 (2021).

[12]J. Lather, A. N. K. Thabassum, J. Singh, and J. George, "Cavity catalysis: Modifying linear free-energy relationship under cooperative vibrational strong coupling," Chem. Sci. **13**, 195–202 (2022).

[13]A. Thomas, J. George, A. Shalabney, M. Dryzhakov, S. J. Varma, J. Moran, T. Chervy, X. Zhong, E. Devaux, C. Genet, J. A. Hutchison, and T. W. Ebbesen, "Ground-state chem-

ical reactivity under vibrational coupling to the vacuum electromagnetic field," Angew. Chem. Int. Ed. **55**, 11462–11466 (2016).

[14]R. M. A. Vergauwe, A. Thomas, K. Nagarajan, A. Shalabney, J. George, T. Chervy, M. Seidel, E. Devaux, V. Torbeev, and T. W. Ebbesen, "Modification of enzyme activity by vibrational strong coupling of water," Angew. Chem. Int. Ed. **58**, 15324–15328 (2019).

[15]A. Thomas, L. Lethuillier-Karl, K. Nagarajan, R. M. A. Vergauwe, J. George, T. Chervy, A. Shalabney, E. Devaux, C. Genet, J. Moran, and T. W. Ebbesen, "Tilting a ground-state reactivity landscape by vibrational strong coupling," Science **363**, 615–619 (2019).

[16]Y. Pang, A. Thomas, K. Nagarajan, R. M. A. Vergauwe, K. Joseph, B. Patrahau, K. Wang, C. Genet, and T. W. Ebbesen, "On the role of symmetry in vibrational strong coupling: The case of charge-transfer complexation," Angew. Chem. Int. Ed. **59**, 10436–10440 (2020).

[17]A. Sau, K. Nagarajan, B. Patrahau, L. Lethuillier-Karl, R. M. A. Vergauwe, A. Thomas, J. Moran, C. Genet, and T. W. Ebbesen, "Modifying Woodward-Hoffmann stereoselectivity under vibrational strong coupling," Angew. Chem. Int. Ed. **60**, 5712–5717 (2021).

[18]A. Shalabney, J. George, J. Hutchison, G. Pupillo, C. Genet, and T. W. Ebbesen, "Coherent coupling of molecular resonators with a microcavity mode," Nat. Commun. **6**, 5981 (2015).

[19]A. D. Dunkelberger, B. T. Spann, K. P. Fears, B. S. Simpkins, and J. C. Owrutsky, "Modified relaxation dynamics and coherent energy exchange in coupled vibration-cavity polaritons," Nat. Commun. **7**, 13504 (2016).

[20]A. B. Grafton, A. D. Dunkelberger, B. S. Simpkins, J. F. Triana, F. J. Hernández, F. Herrera, and J. C. Owrutsky, "Excited-state vibration-polariton transitions and dynamics in nitroprusside," Nat. Commun. **12**, 214 (2021).

[21]R. Duan, J. N. Mastron, Y. Song, and K. J. Kubarych, "Isolating polaritonic 2D-IR transmission spectra," J. Phys. Chem. Lett. **12**, 11406–11414 (2021).

[22]B. Cohn, S. Sufrin, and L. Chuntonov, "Ultrafast vibrational excitation transfer on resonant antenna lattices revealed by two-dimensional infrared spectroscopy," J. Chem. Phys. **156**, 121101 (2022).

[23]G. Stemo, J. Nishiuchi, H. Bhakta, H. Mao, G. Wiesehan, W. Xiong, and H. Katsuki, "Ultrafast spectroscopy under vibrational strong coupling in diphenylphosphoryl azide," J. Phys. Chem. A **128**, 1817–1824 (2024).

[24]A. Shalabney, J. George, H. Hiura, J. A. Hutchison, C. Genet, P. Hellwig, and T. W. Ebbesen, "Enhanced Raman scattering from vibro-polariton hybrid states," Angew. Chem. Int. Ed. **54**, 7971–7975 (2015).

[25]W. M. Takele, L. Piatkowski, F. Wackenhut, S. Gawinkowski, A. J. Meixner, and J. Waluk, "Scouting for strong light-matter coupling signatures in Raman spectra," Phys. Chem. Chem. Phys. **23**, 16837–16846 (2021).

[26]K. S. Menghrajani, M. Chen, K. Dholakia, and W. L. Barnes, "Probing vibrational strong coupling of molecules with wavelength-modulated Raman spectroscopy," Adv. Opt. Mater. **10**, 2102065 (2022).

[27]F. Verdelli, J. J. P. M. Schulpen, A. Baldi, and J. G. Rivas, "Chasing vibro-polariton fingerprints in infrared and Raman spectra using surface lattice resonances on extended metasurfaces," J. Phys. Chem. C **126**, 7143–7151 (2022).

[28]M. Ruggenthaler, J. Flick, C. Pellegrini, H. Appel, I. V. Tokatly, and A. Rubio, "Quantum-electrodynamical density-functional theory: Bridging quantum optics and electronic-structure theory," Phys. Rev. A **90**, 012508 (2014).

[29]J. Flick, D. M. Welakuh, M. Ruggenthaler, H. Appel, and A. Rubio, "Light-matter response in nonrelativistic quantum electrodynamics," ACS Photonics **6**, 2757–2778 (2019).

[30]J. Yang, Q. Ou, Z. Pei, H. Wang, B. Weng, Z. Shuai, K. Mullen, and Y. Shao, "Quantum-electrodynamical time-dependent density functional theory within Gaussian atomic basis," J. Chem. Phys. **155**, 064107 (2021).

[31]J. McTague and I. Foley, Jonathan J., "Non-Hermitian cavity quantum electrodynamics-configuration interaction singles approach for polaritonic structure with *ab initio* molecular Hamiltonians," J. Chem. Phys. **156**, 154103 (2022).

[32]N. Vu, G. M. McLeod, K. Hanson, and A. E. I. DePrince, "Enhanced diastereocontrol via strong light-matter interactions in an optical cavity," J. Phys. Chem. A **126**, 9303–9312 (2022).

[33]T. S. Haugland, E. Ronca, E. F. Kjønstad, A. Rubio, and H. Koch, "Coupled cluster theory for molecular polaritons: Changing ground and excited states," Phys. Rev. X **10**, 041043 (2020).

[34]U. Mordovina, C. Bungey, H. Appel, P. J. Knowles, A. Rubio, and F. R. Manby, "Polaritonic coupled-cluster theory," Phys. Rev. Res. **2**, 023262 (2020).

[35]M. Castagnola, R. R. Riso, A. Barlini, E. Ronca, and H. Koch, "Polaritonic response theory for exact and approximate wave functions," WIREs Comput. Mol. Sci. **14**, e1684 (2024).

[36]J. Flick, M. Ruggenthaler, H. Appel, and A. Rubio, "Atoms and molecules in cavities, from weak to strong coupling in quantum-electrodynamics (QED) chemistry," Proc. Natl. Acad. Sci. U.S.A. **114**, 3026–3034 (2017).

[37]J. Flick, H. Appel, M. Ruggenthaler, and A. Rubio, "Cavity Born-Oppenheimer approximation for correlated electron-nuclear-photon systems," J. Chem. Theory Comput. **13**, 1616–1625 (2017).

[38]T. E. Li, J. E. Subotnik, and A. Nitzan, "Cavity molecular dynamics simulations of liquid water under vibrational ultrastrong coupling," Proc. Natl. Acad. Sci. U.S.A. **117**, 18324–18331 (2020).

[39]E. W. Fischer and P. Saalfrank, "Ground state properties and infrared spectra of anharmonic vibrational polaritons of small molecules in cavities," J. Chem. Phys. **154**, 104311 (2021).

[40]J. Bonini and J. Flick, "*Ab initio* linear-response approach to vibro-polaritons in the cavity Born-Oppenheimer approximation," J. Chem. Theory Comput. **18**, 2764–2773 (2022).

[41]T. Schnappinger, D. Sidler, M. Ruggenthaler, A. Rubio, and M. Kowalewski, "Cavity Born-Oppenheimer Hartree-Fock ansatz: Light-matter properties of strongly coupled molecular ensembles," J. Phys. Chem. Lett. **14**, 8024–8033 (2023).

[42]T. Schnappinger and M. Kowalewski, "*Ab initio* vibro-polaritonic spectra in strongly coupled cavity-molecule systems," J. Chem. Theory Comput. **19**, 9278–9289 (2023).

[43]S. Angelico, T. S. Haugland, E. Ronca, and H. Koch, "Coupled cluster cavity Born-Oppenheimer approximation for electronic strong coupling," J. Chem. Phys. **159**, 214112 (2023).

[44]M. R. Fiechter and J. O. Richardson, "Understanding the cavity Born-Oppenheimer approximation," J. Chem. Phys. **160**, 184107 (2024).

[45]E. W. Fischer and P. Saalfrank, "Beyond cavity Born-Oppenheimer: On nonadiabatic coupling and effective ground state Hamiltonians in vibro-polaritonic chemistry," J. Chem. Theory Comput. **19**, 7215–7229 (2023).

[46]E. W. Fischer, J. A. Syska, and P. Saalfrank, "A quantum chemistry approach to linear vibro-polaritonic infrared spectra with perturbative electron-photon correlation," J. Phys.

Chem. Lett. **15**, 2262–2269 (2024).

[47]M. Head-Gordon, "Quantum chemistry and molecular processes," J. Phys. Chemi. **100**, 13213–13225 (1996).

[48]Y. Yamaguchi, Y. Osamura, J. D. Goddard, and H. F. Schaefer III, *A new dimension to quantum chemistry: Analytical derivative methods in ab-initio molecular elctronic structure theory*, The international series of monographs on chemistry (Oxford University Press, Oxford, 1994) p. 471.

[49]Y. Yamaguchi and H. F. Schaefer III, "Analytic derivative methods in molecular electronic structure theory: A new dimension to quantum chemistry and its applications to spectroscopy," in *Handbook of High-resolution Spectroscopy* (John Wiley & Sons, Ltd, 2011).

[50]W. Liang, Z. Pei, Y. Mao, and Y. Shao, "Evaluation of molecular photophysical and photochemical properties using linear response time-dependent density functional theory with classical embedding: Successes and challenges," J. Chem. Phys. **156**, 210901 (2022).

[51]D. Chen, J. Liu, H. Ma, Q. Zeng, and W. Liang, "Analytical derivative techniques for TDDFT excited-state properties: Theory and application," Sci. China Chem. **57**, 48–57 (2014).

[52]T. Schnappinger and M. Kowalewski, "Do Molecular Geometries Change Under Vibrational Strong Coupling?" J. Phys. Chem. Lett. , 7700–7707 (2024).

[53]J. J. Foley, J. F. McTague, and A. E. DePrince, "*Ab initio* methods for polariton chemistry," Chem. Phys. Rev. **4**, 041301 (2023).

[54]V. Rokaj, D. M. Welakuh, M. Ruggenthaler, and A. Rubio, "Light-matter interaction in the long-wavelength limit: No ground-state without dipole self-energy," J. Phys. B: At. Mol. Opt. Phys. **51**, 034005 (2018).

[55]T. Helgaker, "Gradient theory," in *Encyclopedia of Computational Chemistry* (John Wiley & Sons, Ltd, 2002).

[56]J. A. Pople, R. Krishnan, H. B. Schlegel, and J. S. Binkley, "Derivative studies in Hartree-Fock and Møller-Plesset theories," Int. J. Quantum Chem. **16**, 225–241 (1979).

[57]D. R. Maurice, *Single Electron Theories of Excited States*, Ph.D Thesis, University of California, Berkeley (1998).

[58]T. Helgaker, S. Coriani, P. Jørgensen, K. Kristensen, J. Olsen, and K. Ruud, "Recent advances in wave function-based methods of molecular-property calculations," Chem. Rev. **112**, 543–631 (2012).

[59]Z. Pei, Y. Mao, Y. Shao, and W. Liang, "Analytic high-order energy derivatives for metal nanoparticle-mediated infrared and Raman scattering spectra within the framework of quantum mechanics/molecular mechanics model with induced charges and dipoles," J. Chem. Phys. **157**, 164110 (2022).

[60]E. Wilson, J. Decius, and P. Cross, *Molecular Vibrations: The Theory of Infrared and Raman Vibrational Spectra* (Dover Publications, 1980).

[61]J. Neugebauer, M. Reiher, C. Kind, and B. A. Hess, "Quantum chemical calculation of vibrational spectra of large molecules—Raman and IR spectra for Buckminsterfullerene," J. Comput. Chem. **23**, 895–910 (2002).

[62]E. Epifanovsky, A. T. B. Gilbert, X. Feng, J. Lee, Y. Mao, N. Mardirossian, P. Pokhilko, A. F. White, M. P. Coons, A. L. Dempwolff, Z. Gan, D. Hait, P. R. Horn, L. D. Jacobson, I. Kaliman, J. Kussmann, A. W. Lange, K. U. Lao, D. S. Levine, J. Liu, S. C. McKenzie, A. F. Morrison, K. D. Nanda, F. Plasser, D. R. Rehn, M. L. Vidal, Z.-Q. You, Y. Zhu, B. Alam, B. J. Albrecht, A. Aldossary, E. Alguire, J. H. Andersen, V. Athavale, D. Barton, K. Begam, A. Behn, N. Bellonzi, Y. A. Bernard, E. J. Berquist, H. G. A. Burton, A. Carreras, K. Carter-Fenk, R. Chakraborty, A. D. Chien, K. D. Closser, V. Cofer-Shabica, S. Dasgupta, M. de Wergifosse, J. Deng, M. Diedenhofen, H. Do, S. Ehlert, P.-T. Fang, S. Fatehi, Q. Feng, T. Friedhoff, J. Gayvert, Q. Ge, G. Gidofalvi, M. Goldey, J. Gomes, C. E. González-Espinoza, S. Gulania, A. O. Gunina, M. W. D. Hanson-Heine, P. H. P. Harbach, A. Hauser, M. F. Herbst, M. Hernández Vera, M. Hodecker, Z. C. Holden, S. Houck, X. Huang, K. Hui, B. C. Huynh, M. Ivanov, A. Jász, H. Ji, H. Jiang, B. Kaduk, S. Kähler, K. Khistyaev, J. Kim, G. Kis, P. Klunzinger, Z. Koczor-Benda, J. H. Koh, D. Kosenkov, L. Koulias, T. Kowalczyk, C. M. Krauter, K. Kue, A. Kunitsa, T. Kus, I. Ladjánszki, A. Landau, K. V. Lawler, D. Lefrancois, S. Lehtola, R. R. Li, Y.-P. Li, J. Liang, M. Liebenthal, H.-H. Lin, Y.-S. Lin, F. Liu, K.-Y. Liu, M. Loipersberger, A. Luenser, A. Manjanath, P. Manohar, E. Mansoor, S. F. Manzer, S.-P. Mao, A. V. Marenich, T. Markovich, S. Mason, S. A. Maurer, P. F. McLaughlin, M. F. S. J. Menger, J.-M. Mewes, S. A. Mewes, P. Morgante, J. W. Mullinax, K. J. Oosterbaan, G. Paran, A. C. Paul, S. K. Paul, F. Pavošević, Z. Pei, S. Prager, E. I. Proynov, A. Rák, E. Ramos-Cordoba, B. Rana, A. E. Rask, A. Rettig, R. M. Richard, F. Rob, E. Rossomme, T. Scheele, M. Scheurer, M. Schneider, N. Sergueev, S. M. Sharada, W. Skomorowski, D. W. Small, C. J. Stein, Y.-C. Su, E. J. Sundstrom, Z. Tao, J. Thirman, G. J. Tornai, T. Tsuchimochi, N. M.

Tubman, S. P. Veccham, O. Vydrov, J. Wenzel, J. Witte, A. Yamada, K. Yao, S. Yeganeh, S. R. Yost, A. Zech, I. Y. Zhang, X. Zhang, Y. Zhang, D. Zuev, A. Aspuru-Guzik, A. T. Bell, N. A. Besley, K. B. Bravaya, B. R. Brooks, D. Casanova, J.-D. Chai, S. Coriani, C. J. Cramer, G. Cserey, I. DePrince, A. Eugene, J. DiStasio, Robert A., A. Dreuw, B. D. Dunietz, T. R. Furlani, I. Goddard, William A., S. Hammes-Schiffer, T. Head-Gordon, W. J. Hehre, C.-P. Hsu, T.-C. Jagau, Y. Jung, A. Klamt, J. Kong, D. S. Lambrecht, W. Liang, N. J. Mayhall, C. W. McCurdy, J. B. Neaton, C. Ochsenfeld, J. A. Parkhill, R. Peverati, V. A. Rassolov, Y. Shao, L. V. Slipchenko, T. Stauch, R. P. Steele, J. E. Subotnik, A. J. W. Thom, A. Tkatchenko, D. G. Truhlar, T. Van Voorhis, T. A. Wesolowski, K. B. Whaley, I. Woodcock, H. Lee, P. M. Zimmerman, S. Faraji, P. M. W. Gill, M. Head-Gordon, J. M. Herbert, and A. I. Krylov, "Software for the frontiers of quantum chemistry: An overview of developments in the Q-Chem 5 package," J. Chem. Phys. **155**, 084801 (2021).

[63]V. N. Staroverov, G. E. Scuseria, J. Tao, and J. P. Perdew, "Comparative assessment of a new nonempirical density functional: Molecules and hydrogen-bonded complexes," J. Chem. Phys. **119**, 12129–12137 (2003).

[64]T. Yanai, D. P. Tew, and N. C. Handy, "A new hybrid exchange–correlation functional using the Coulomb-attenuating method (CAM-B3LYP)," Chem. Phys. Lett. **393**, 51–57 (2004).

[65]M. D. Liebenthal and A. E. DePrince, "The orientation dependence of cavity-modified chemistry," J. Chem. Phys. **161**, 064109 (2024).

[66]S. Deng, J. Yang, Y. Shao, Q. Ou, and Z. Shuai, "Optical emission spectra of molecular excitonic polariton computed at the first-principles level QED-TDDFT," ChemPhotoChem , e202400117 (2024).

[67]T. Vreven, M. J. Frisch, K. N. Kudin, H. B. Schlegel, and K. Morokuma, "Geometry optimization with QM/MM methods II: Explicit quadratic coupling," Mol. Phys. **104**, 701–714 (2006).

[68]P. J. Stephens, F. J. Devlin, C. F. Chabalowski, and M. J. Frisch, "*Ab initio* calculation of vibrational absorption and circular dichroism spectra using density functional force fields," J. Phys. Chem. **98**, 11623–11627 (1994).

[69]R. A. Kendall, J. Dunning, Thom H., and R. J. Harrison, "Electron affinities of the first-row atoms revisited. Systematic basis sets and wave functions," J. Chem. Phys. **96**, 6796–6806 (1992).

[70]J. P. Perdew, K. Burke, and M. Ernzerhof, "Generalized gradient approximation made simple," Phys. Rev. Lett. **77**, 3865–3868 (1996).

[71]N. Mardirossian and M. Head-Gordon, "ωB97X-V: A 10-parameter, range-separated hybrid, generalized gradient approximation density functional with nonlocal correlation, designed by a survival-of-the-fittest strategy," Phys. Chem. Chem. Phys. **16**, 9904–9924 (2014).

[72]D. Hait and M. Head-Gordon, "How accurate is density functional theory at predicting dipole moments? An assessment using a new database of 200 benchmark values," J. Chem. Theory Comput. **14**, 1969–1981 (2018).

[73]K. P. Huber and G. Herzberg, *Molecular Spectra and Molecular Structure* (Springer New York, NY, 2013).

[74]X. K. Huang and W. Z. Liang, "Analytical derivative approaches for vibro-polaritionic structures and properties II: Characterizing the IR and Raman spectra of vibro-polaritons," J. Chem. Phys. , submitted (2024).